M.; Nogues, P.; Sentman, R. C. *Tetrahedron Lett.* **1982**, *23*, 603.
12. Hall, Jr. H. K.; Padias, A. B. *Acc. Chem. Res.* **1990**, *23*, 3.
13. Kresel, M.; Garbratski, U.; Kohn. D. H. *J. Polym. Sci., Part A* **1964**, *2*, 105.
14. Gilath, A.; Ronel, S. H.; Shmueli, M.; Kohn, D. H. *J. Appl. Polym. Sci.* **1970**, *14*, 1491.
15. Ronel, S. H.; Shmueli, M.; Kohn, D. H. *J. Polym. Sci., A-1* **1969**, *7*, 2209.
16. Lieberson, A.; Kohn, D. H. *J. Polym. Sci., Polym. Chem. Ed.* **1974**, *12*, 2435.
17. Kharas, G.; Kohn, D. H. *J. Polym. Sci., Polym. Chem. Ed.* **1983**, *21*, 1457.
18. Kharas, G.; Kohn, D. H. *J. Polym. Sci., Polym. Chem. Ed.* **1984**, *22*, 583.
19. Angelorici, M. M.; Kohn, D. H. *J. Appl. Polym. Sci.* **1990**, *40*, 485.
20. Moore, A. H. F. *Org. Syn. Coll. Vol. 4* **1963**, 84.
21. Griffin, A. C.; Bhatti, A. M.; Hung, R. S. in Prasad, P. N.; Ulrich, D. R. Eds. *Nonlinear Optical and Electroactive Polymers*; Plenum Press: New York, 1987, pp 375-391.
22. Corson, B. B.; Stoughton, R. W. *J. Am. Chem. Soc.* **1928**, *50*, 2825.
23. Lee, J.-Y. *Polym. Bull.* **1994**, *33*, 635.

The Equilibrium between Dilatant and Thixotropic Flow Units

Jeong-Hwan Bang, Nam-Jeong Kim†, Sang-Won Choi‡, Eung-Ryul Kim§, and Sang-Joon Hahn§

Department of Chemistry, Seonam University, Namwon, Chonbuk 590-170, Korea
†Department of Chemistry, Sahmyook University, Seoul 139-742, Korea
§Department of Chemical Engineering, Yosu National Fisheries University, Yosu, Chonnam 550-749, Korea
§Department of Chemistry, Hanyang University, Seoul 133-791, Korea
Received November 7, 1995

Flow properties of all suspensions are controlled by their flow units. The factors effecting on the flow units are the characteristics of the particle itself (surface properties, particle sizes, particle shapes and etc.), the electrostatic interactions among the particles and the influences of the medium in the suspensions. Here, we studied the transition between the flow units with shear rate which can be added to the above factors. For the concentrated starch-water suspensions, by using the Couette type rotational viscometer, we confirmed that at low shear rate, dilatancy is appeared, but it is transformed to thixotropy with increasing shear rate. In order to explain this fact, we derived the following flow equation, representing the transition from dilatancy to thixotropy with shear rate, by assuming the equilibrium between the flow units.

$$f=\frac{X_1\beta_1}{\alpha_1}\dot{s} + \frac{1}{1+K\ \exp(c_0\dot{s}^2/RT)}\frac{1-X_1}{\alpha_2}\sinh^{-1}\{(\beta_2)_0\ \dot{s}\ \exp(c_2\dot{s}^2/RT)\} + \frac{K\ \exp(c_0\dot{s}^2/RT)}{1+K\ \exp(c_0\dot{s}^2/RT)}\frac{1-X_1}{\alpha_3}\sinh^{-1}\{(\beta_3)_0\ \dot{s}\ \exp(-c_3\dot{s}^2/RT)\}$$

By applying this flow equation to the experimental flow curves for the concentrated starch-water suspensions, the flow parameters were obtained. And, by substituting the obtained flow parameters to the flow equation, the theoretical flow curves were reproduced. Also, Ostwald curve was represented by applying the flow equation, and the applicability for stress relaxation was discussed.

Introduction

Most of the suspensions exhibit complicated non-Newtonian flow, such as thixotropy and dilatancy, by the process of the structural change among the particles with applied shear. These phenomena have been studied by many rheologists with the interests in views of the industrial applicability and the pure science. Here, the investigations for these phenomena will be reviewed and the objectives in this paper will also be given.

Thixotropy is a common phenomenon, and is important in the paint, cosmetic and food industries. Recently, thixotropy is found in the fields of biochemistry and material science.

†All correspondence should be addressed here.

Generally, thixotropy is defined it as a time-dependent shear-thinning phenomenon. And, Hahn *et al.*[1] have defined as the phenomenon having the following characteristics, (1) it accompanies structural change brought about by applying mechanical disturbance to a system, (2) when the mechanical disturbance is removed, the system recovers its original structure, and (3) the flow curve (shear rate *vs.* shear stress) of the system shows a hysteresis loop.

There are two main streams in the theoretical interpretations of thixotropic phenomena. One is Goodeave's network theory[2] and the other is Ree-Eyring's kinetic theory. In 1955, by developing Eyring's theory of transport phenomena,[3] the generalized viscosity formula known as the Ree-Eyring equation[4] was derived. In 1957, Hahn *et al.*[5] have applied the generalized viscosity formula to the thixotropic hysteresis.

Many other investigators have developed their own theories with constitutive equations of inelastic viscous fluids. By developing the kinetic theory, Park and Ree[6] have proposed an elaborate theory which was successfully applied to bentonite suspensions and Utsugi and Ree[7] have studied the Ostwald curves which were related to thixotropy, and have showed that their equation of flow was related with the Einstein equation of flow. Recently, Sohn *et al.*[8] have suggested a modified and simple thixotropic equation which was derived by introducing the concept of structural change caused by shear into the Ree-Eyring equation of flow.

As well as thixotropy, dilatancy is quite frequently encountered in pigment-vehicle suspensions such as paints and printing inks. It has been stated that dilatancy is the opposite of thixotropy because not only does a dilatant material increase its resistance to flow in a nonlinear way as the rate of shear increases, but also the suspended particles, unlike those in thixotropic materials, are dispersed usually possessing vigorous Brownian motion and showing no sign of flocculation. Many empirical or semi-empirical approaches have been attempted to represent the flow behavior of shear-thickening materials, which increase the viscosity as the rate of shear increases.

Hoffman[9] has studied dilatant viscosity behavior in concentrated suspensions of monosized spheres of polymeric resin. The analysis was carried out on the presumption that the dominant forces leading to the flow instability are the van der Waals-London attraction, electric double layer repulsion and the shear stress between ordered layers of spheres. He has pointed out that the latter two forces are more significant than the first one.

Kanno and Umeya[10] have observed separately that TiO_2-water suspension behaved as dilatant system. They have observed that the viscosity of the suspension has shown notable increase with the increase in the concentration as well as in shear rate in the TiO_2 aqueous suspension.

As for the flow mechanism of thixotropic system, many studies have been published. However, in case of dilatant systems, not many theoretical interpretations are available. Bang *et al.*[11] have suggested a dilatant equation which was based on the Ree-Eyring theory and have applied it in the starch-water suspensions.

On the other hand, there are frequent cases where thixotropy and dilatancy occur in the same flow system. In the clay-water suspension, Green[12] has discovered that the suspension displayed both thixotropy and dilatancy. Also, we have found that the concentrated starch-water suspensions showed the flow transition from dilatancy to thixotropy with applied shear.

In this paper, we studied the mechanism that the flow transition was occurred from dilatancy to thixotropy with increasing shear rate by assuming an equilibrium between dilatant and thixotropic flow units for the concentrated starch-water suspensions. We present here the experimental results thus far obtained, and the theoretical explanation of the results. And, we discussed the flow parameters, the Ostwald curve and the stress relaxation.

Theory

Generalized Flow Equation (Ree-Eyring Theory[4]): According to Eyring's equation of shear flow[3], the rate of shear is given as

$$\dot{s}=(\lambda/\lambda_1)_n 2k_n \sinh \alpha_n f_n \tag{1}$$

where, $\dot{s}$ is the rate of shear, f_n is the shear stress, k_n is the rate constant for the flow process of a unit which belongs to the n-th group of units, $\alpha_n=(\lambda\lambda_2\lambda_3)_n/(2kT)$, λ_1, λ_2, λ_3 and λ are the molecular parameters, and the subscript n and the parentheses indicate that the inside quantities belong to a flow unit of n-th group.

The stress acting on the units of n-th group is $X_n f_n$; thus, stress f is

$$f=\sum_{n=1}^{N} X_n f_n \tag{2}$$

where X_n is the mole fraction of the n-th group. If one introduces f_n from Eq. (1) into Eq. (2), the following equation results:

$$f=\sum_{n=1}^{N} \frac{X_n}{\alpha_n} / \sinh^{-1}(\beta_n \dot{s}) \tag{3}$$

where $\beta_n=1/\{(\lambda/\lambda_1)_n 2k_n\}$, which is proportional to the relaxation time of the n-th group.

Newtonian Unit[4]. Rewriting Eq. (3) gives

$$f=\sum_{n=1}^{N} \frac{X_n \beta_n \dot{s}}{\alpha_n} \frac{\sinh^{-1}(\beta_n \dot{s})}{\beta_n \dot{s}} \tag{4}$$

From the property of the function, $(\sinh^{-1}X)/X$, Eq. (5) is obtained.

$$\lim_{\beta_n \to 0} \frac{\sinh^{-1}(\beta_n \dot{s})}{\beta_n \dot{s}}=1 \tag{5}$$

The unit 1 for the condition, $\beta_n \dot{s} \ll 1$, behaves as a Newtonian unit; *i.e.*, the stress on Newtonian unit f_1 is

$$f_1=(X_1\beta_1/\alpha_1)\dot{s} \tag{6}$$

Non-Newtonian Units[8,11]. It is assumed that there is a structural change according to the increased shear rate. If the structural change occurs, the corresponding work has to be done by the shear. The work needed for the structural change is strain energy, ω_n. The strain energy is calculated by following equation[1]:

$$\omega_n=\int_0^{S_n} f_n \, dS=\int_0^{S_n} G_n S \, dS=G_n(\gamma_n \dot{s})^2/2k_{f_n}{}^2$$
$$=c_n \dot{s}^2 \tag{7}$$

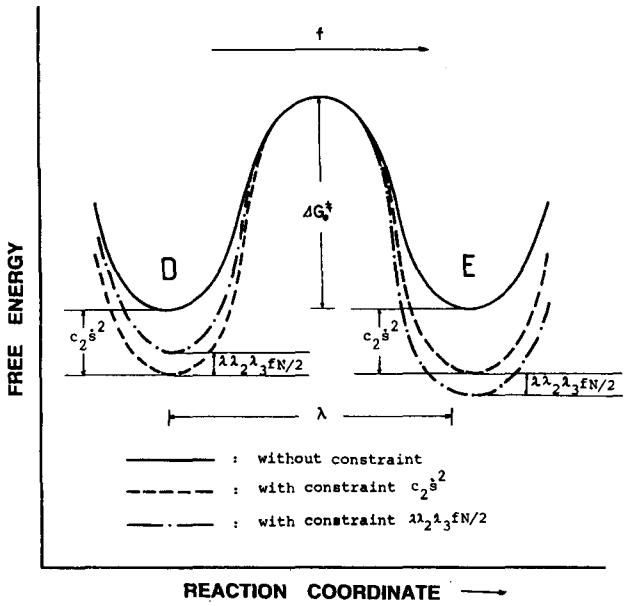

Figure 1. The activation free energy curves of flow unit 2.

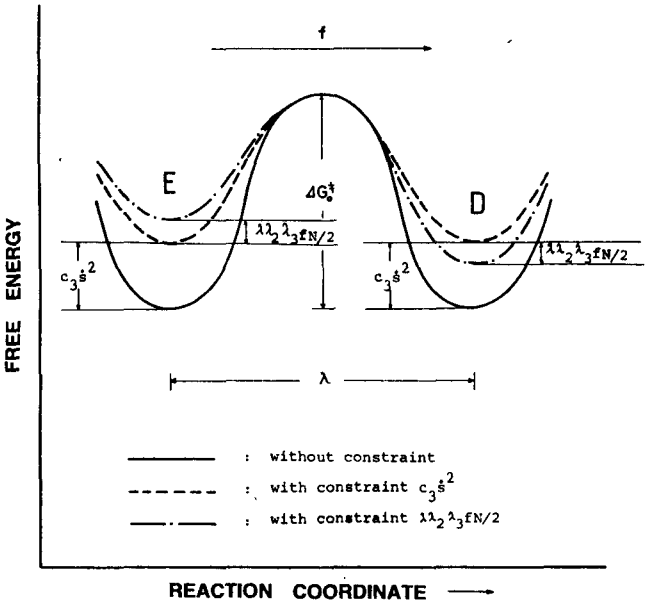

Figure 2. The activation free energy curves of flow unit 3.

Here, G_n is the spring constant of the n-th group, and S_n is the molecular displacement at which the structural change occurs, where $S_n=\gamma_n\dot{s}/k_{f_n}$, γ_n being a proportional constant and k_{f_n} being the rate constant for f_n. The latter relation is obtained from the assumption that the molecular or granular displacement per unit time forced by the shear stress is directly proportional to the shear rate.

The strain energy changes accompanied by the structural change, disentanglement (D) $\rightleftarrows$ entanglement (E), will contribute to the activation free energy of flow. In the flow process which is simultaneously accompanied by the structural change, D→E, the activation free energy of flow is increased by the amount of strain energy, ω_2. Thus, the rate constant, k_n, for unit 2 becomes[11]

$$k_2=\frac{kT}{h}\exp\left\{-\left(\frac{\Delta G^{\neq}+c_2\dot{s}^2}{RT}\right)\right\}$$
$$=k_0\exp\left(\frac{-c_2\dot{s}^2}{RT}\right) \tag{8}$$

where k_0 is the rate constant for the flow unit when there is no constraint. Here the free energy diagram shown in Figure 1 is assumed for the jumping process, *i.e.*, the energy of activation is increased by ω_2 compared to that when there is no constraint. This is natural since the flow becomes harder by a shear stress, *i.e.*, the energy of the activation is increased by the forced entanglement. Thus, the relaxation time (β_2) is

$$\beta_2=(\beta_2)_0\exp\left(\frac{c_2\dot{s}^2}{RT}\right) \tag{9}$$

where $(\beta_2)_0=\frac{1}{2}\left(\frac{\lambda_1}{\lambda}\right)_2\frac{1}{k_0}=\frac{1}{2}\left(\frac{\lambda_1}{\lambda}\right)_2\frac{h}{kT}\exp(\Delta G^{\neq}/RT)$ (10)

Rewritten Eq. (3) for the unit 2, the shear stress (f_2) on the structural change, D→E, is obtained:

$$f_2=\frac{X_2}{\alpha_2}\sinh^{-1}\{(\beta_2)_0\dot{s}\exp(c_2\dot{s}^2/RT)\} \tag{11}$$

While, in the flow process which is simultaneously accompanied by the structural change, E→D, the activation free energy of flow is decreased by the amount of strain energy, ω_3. Thus, the rate constant, k_3 becomes[8]

$$k_3=\frac{kT}{h}\exp\left\{-\left(\frac{\Delta G^{\neq}-c_3\dot{s}^2}{RT}\right)\right\}$$
$$=k_0\exp\left(\frac{c_3\dot{s}^2}{RT}\right) \tag{12}$$

Here the free energy diagram shown in Figure 2 is assumed for the jumping process, *i.e.*, the energy of the activation is decreased by ω_3 compared to that when there is no constraint. This is natural since the flow becomes softer by a shear stress, *i.e.*, the energy of the activation is decreased by the forced disentanglement. Thus, the relaxation time (β_3) is

$$\beta_3=(\beta_3)_0\exp\left(\frac{-c_3\dot{s}^2}{RT}\right) \tag{13}$$

where $(\beta_3)_0=\frac{1}{2}\left(\frac{\lambda_1}{\lambda}\right)_3\frac{1}{k_0}=\frac{1}{2}\left(\frac{\lambda_1}{\lambda}\right)_3\frac{h}{kT}\exp(\Delta G^{\neq}/RT)$ (14)

Rewritten Eq. (3) for the unit 3, the shear stress (f_3) on the structural change, E→D, is obtained:

$$f_3=\frac{X_3}{\alpha_3}\sinh^{-1}\{(\beta_3)_0\dot{s}\exp(-c_3\dot{s}^2/RT)\} \tag{15}$$

Derivation of General Flow Equation Involved in Flow Unit Transition. Hahn *et al.*[5] had considered entanglement-disentanglement transition for thixotropic system. We consider the case where flow unit 2 and flow unit 3 are in kinetic equilibrium, flow unit 2 $\rightleftharpoons$ flow unit 3. The equilibrium is moved by the strain energy, ω_0, stored up on the flow unit as shown in Figure 3. Then, the net rate of transition is given by

$$-\frac{dX_2}{dt}=X_2k_f\exp(\mu c_0\dot{s}^2/kT)-X_3k_b\exp\{-(1-\mu)c_0\dot{s}^2/kT\} \tag{16}$$

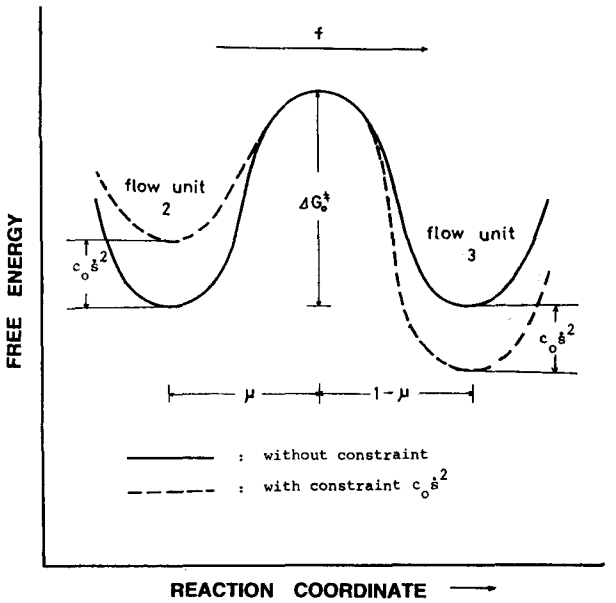

Figure 3. The activation free energy curves for transition, flow unit 2 ⇌ flow unit 3.

For a symmetrical barrier, μ being the coefficient of energy barrier is one-half. k_f and k_b are the rate constants for the forward and backward reaction at zero stress, respectively.

Here we apply the steady state approximation and obtain

$$X_2=\frac{1}{1+K\ \exp(c_0\dot{s}^2/RT)}(1-X_1) \tag{17}$$

and

$$X_3=\frac{K\ \exp(c_0\dot{s}^2/kT)}{1+K\ \exp(c_0\dot{s}^2/RT)}(1-X_1) \tag{18}$$

where the following relations were introduced:

$$K=k_f/k_b \tag{19}$$

$$X_1+X_2+X_3=1 \tag{20}$$

In Eq. (19), K is the equilibrium constant at zero stress. Then, we consider that total shear stress is the sum of f_1, f_2 and f_3: *i.e.*, from Eq. (6), (11) and (15), total shear stress is

$$f=\frac{X_1\beta_1}{\alpha_1}\dot{s}+\frac{X_2}{\alpha_2}\sinh^{-1}\{(\beta_2)_0\dot{s}\exp(c_2\dot{s}^2/kT)\}+\frac{X_3}{\alpha_3}\sinh^{-1}\{(\beta_3)_0\dot{s}\ \exp(-c_3\dot{s}^2/kT)\} \tag{21}$$

The substitutions of Eq. (17) and (18) into (21) yield

$$f=\frac{X_1\beta_1}{\alpha_1}\dot{s}+\frac{1}{1+K\ \exp(c_0\dot{s}^2/kT)}\left(\frac{1-X_1}{\alpha_2}\right)\sinh^{-1}\{(\beta_2)_0\dot{s}\exp(c_2\dot{s}^2/kT)\}+\frac{K\ \exp(c_0\dot{s}^2/kT)}{1+K\ \exp(c_0\dot{s}^2/kT)}\left(\frac{1-X_1}{\alpha_3}\right)\sinh^{-1}\{(\beta_3)_0\dot{s}\exp(-c_3\dot{s}^2/kT)\} \tag{22}$$

In the above, we considered the case where the equilibrium between flow unit 2 and flow unit 3 shift to the side of the flow unit 3. Here, the flow unit 2 and the flow unit 3 are treated as being structured unit and being destroyed unit, respectively. Thus, with increasing shear rate the viscosity increases in a region of lower shear rate and decreases in a region of higher shear rate. Transition from dilatancy to thixotropy with applied shear rate exemplifies this case. On the other hand, there is the opposite case where the equilibrium shifts to the side of the flow unit 2. Systems showing this effect are said to show the transition from thixotropy to dilatancy with applied shear rate.

In Eq. (22), we can assume reasonably the following conditions since flow unit transition is reversible: $\alpha_2\cong\alpha_3$. $(\beta_2)_0\cong(\beta_3)_0$ and $c_2\cong c_3$. thus Eq. (22) is

$$f=\frac{X_1\beta_1}{\alpha_1}\dot{s}+\frac{1}{1+K\ \exp(c_0\dot{s}^2/kT)}\left(\frac{1-X_1}{\alpha_2}\right)\sinh^{-1}\{(\beta_2)_0\dot{s}\exp(c_2\dot{s}^2/kT)\}+\frac{K\ \exp(c_0\dot{s}^2/kT)}{1+K\ \exp(c_0\dot{s}^2/kT)}\left(\frac{1-X_1}{\alpha_2}\right)\sinh^{-1}\{(\beta_2)_0\dot{s}\ \exp(-c_2\dot{s}_2/kT)\} \tag{23}$$

Eq. (23) is the general flow equation involved in flow unit transition.

In case of the condensed system where the Newtonian unit's contribution is negligible, Eq. (23) will be simplified as follows:

$$f=\frac{1}{1+K\ \exp(c_0\dot{s}^2/kT)}\left(\frac{1}{\alpha_2}\right)\sinh^{-1}\{(\beta_2)_0\dot{s}\ \exp(c_2\dot{s}^2/kT)\}+\frac{K\ \exp(c_0\dot{s}^2/kT)}{1+K\ \exp(c_0\dot{s}^2/kT)}\left(\frac{1}{\alpha_2}\right)\sinh^{-1}\{(\beta_2)_0\dot{s}\ \exp(-c_2\dot{s}^2/kT)\} \tag{24}$$

Here, $X_1\cong 0$.

Application of the Theory

Experiment. Testing materials were chemically pure corn starch and potato starch which were commercial products of Junsei Chemical Co., Japan, and the average granular size was approximately 5 μm and 30 μm, respectively.

The starch-water suspensions of various concentrations were prepared and the suspensions in 250 mL flasks were stirred for about ten hours at room temperature, and then the flow properties were measured by using the Couette type rotational viscometer[13] built at this laboratory.

The results are presented in Figure 4 to 8. The flow curves are composed of up-curve and down-curve, and show the transition from dilatancy to thixotropy with applied shear rate at up-curve. Here, the flow curve obtained with increasing is called up-curve and in contrary the reverse is called down-curve.

Up-Curve Flow Equation and Down-Curve Flow Equation. For the concentrated systems, Eq. (24) is applicable to the up-curve. And for the down-curve, the following equation is eligible.

$$f=\frac{1}{1+K\ \exp(c_0\dot{s}_m^2/kT)}\left(\frac{1}{\alpha_2}\right)\sinh^{-1}\{(\beta_2)_0\dot{s}\ \exp(c_2\dot{s}^2/kT)\}$$

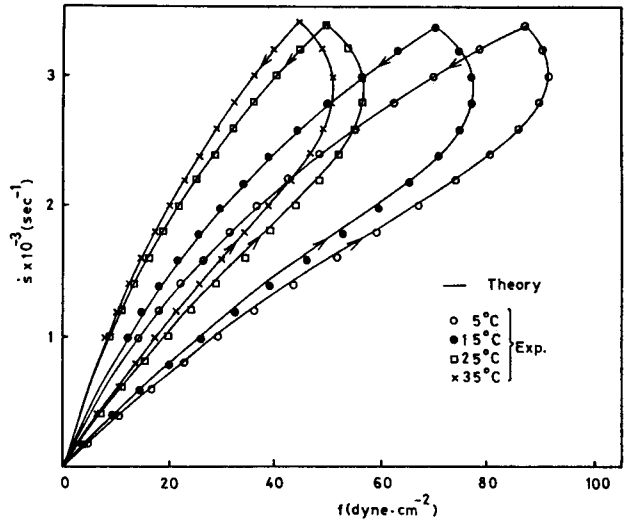

Figure 4. Flow curves of 30 wt.% corn starch-water suspensions with various temperature.

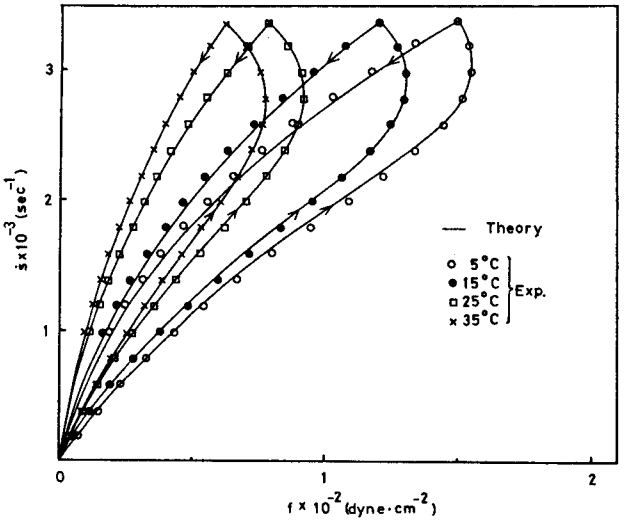

Figure 5. Flow curves of 35 wt.% corn starch-water suspensions with various temperature.

$$+\frac{K\ \exp(c_0\dot{s}_m^2/kT)}{1+K\ \exp(c_0\dot{s}_m^2/kT)}\left(\frac{1}{\alpha_2}\right)\sinh^{-1}\{(\beta_2)_0\dot{s}\ \exp(-c_2\dot{s}_m^2/kT)\} \tag{25}$$

where $\dot{s}_m$ is the shear rate at the apex. The reasons for Eq. (25) are as follows: (1) at the apex, the flow equation is also represented by Eq. (25), (2) all of the parameters in Eq. (25) will not change in the process of the down-curve, and (3) any recovery of deformed structure is negligible and the destruction of the formed structure dominates.

Determination of Parameters. In case of the concentrated starch-water suspensions, at a region of lower shear rate, the process of the entanglement is dominant while the process of the disentanglement is negligible. In Eq. (24), the first term describes the process of the entanglement and the second term describes the process of the disentanglement. Therefore, Eq. (26) is applicable to the region of respectively lower shear rate.

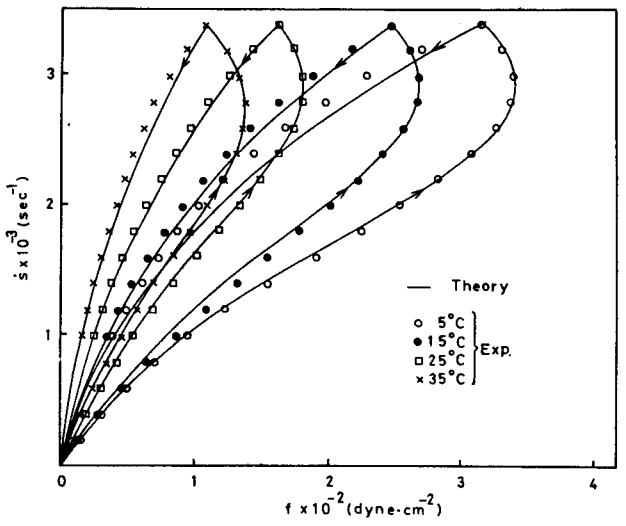

Figure 6. Flow curves of 40 wt.% corn starch-water suspensions with various temperature.

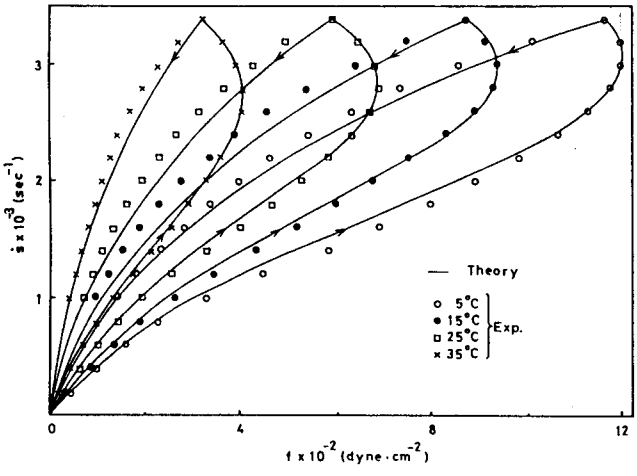

Figure 7. Flow curves of 45 wt.% corn starch-water susepnsions with various temperature.

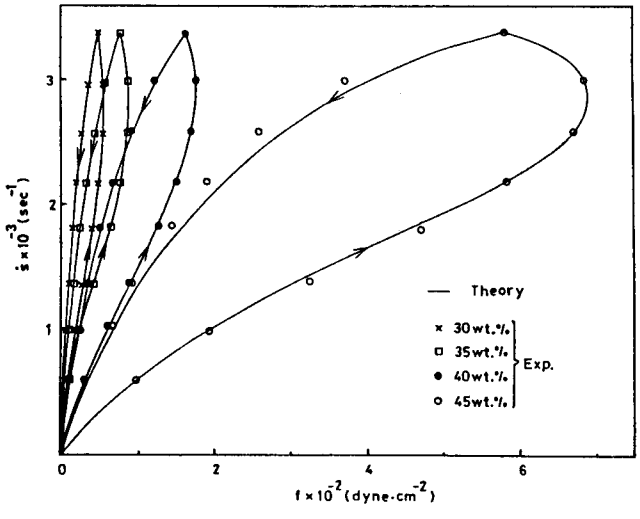

Figure 8. Flow curves of corn starch-water suspensions with various concentrations at 25 ℃.

Table 1. The Values of c_0, K, $(\beta_2)_0$, $1/\alpha_2$ and c_2 for the Corn Starch-Water Suspensions

℃	parameters \ wt.%	30	35	40	45
5	$c_0\times10^4$	1.252	1.234	1.202	1.001
	K×10	.8846	.9161	1.440	2.349
	$(\beta_2)_0\times10^3$	4.40	4.57	9.90	14.3
	$1/\alpha_2$	7.94	9.57	13.4	36.4
	$c_2\times10^3$	.993	1.47	2.91	4.19
15	$c_0\times10^4$	1.519	1.413	1.327	1.302
	K×10³	.6177	.8590	1.112	1.189
	$(\beta_2)_0\times10^3$	3.05	3.16	3.43	9.19
	$1/\alpha_2$	7.93	9.50	13.3	34.0
	$c_2\times10^3$	.843	1.38	2.20	3.12
25	$c_0\times10^4$	1.761	1.753	1.623	1.574
	K×10	.4004	.5142	.5901	.8802
	$(\beta_2)_0\times10^3$	2.47	2.49	4.36	5.30
	$1/\alpha_2$	7.93	9.49	13.0	32.3
	$c_2\times10^3$	.562	.921	1.35	2.48
35	$c_0\times10^4$	2.080	2.068	1.917	1.891
	K×10	.2069	.3134	.5170	.5958
	$(\beta_2)_0\times10^3$	2.17	2.38	2.64	3.76
	$1/\alpha_2$	7.91	9.49	12.9	31.2
	$c_2\times10^3$	.459	.723	1.14	1.49

c_0 and c_2; cal sec^2 mol^{-1}, $1/\alpha_2$: dyne cm^{-2} and $(\beta_2)_0$: sec

$$f=\left(\frac{1}{\alpha_2}\right)\sinh^{-1}\{(\beta_{20}\dot{s}\ \exp(c_2\dot{s}^2/kT)\} \tag{26}$$

The approximation $\sinh^{-1} X\cong\ln 2X$ (for $X\gg1$), is applied to Eq. (26), and the following equation is obtained:

$$f=\frac{1}{\alpha_2}\ln\{2(\beta_2)_0\dot{s}\ \exp(c_2\dot{s}^2/RT)\}$$
$$=\frac{1}{\alpha_2}\left\{\ln\ 2(\beta_2)_0+\ln\ \dot{s}+\frac{c_2\dot{s}^2}{RT}\right\} \tag{27}$$

By applying Eq. (27) to an experimental flow curve, the unknown parameters, $1/\alpha_2$, $(\beta_2)_0$ and c_2 are evaluated.

One should remember that Eq. (24) is composed of two terms with each fraction of flow units. Then, c_0 and K are the determining factors of the fraction. Thus they can be determined by the stress values obtained from a experimental flow curves, at two relevant shear rates.

The results are summarized in Table 1. These parameters were substituted to Eq. (24) and Eq. (25), and the experimental flow curves were reproduced. The results are shown in Figure 4 to 8 by full curve. One notes that the agreement between theory and experiment is good.

Determination of Thermodynamic Parameters for Flow Unit Transition. By plotting ln K *vs.* $1/T$, one obtains the straight lines such as shown in Figure 9. From the slopes of the straight lines, ΔH^os are calculated. Also, ΔG^os are determined from the equation, $\Delta G^o=-RT\ \ln K$. And then, ΔS^os are calculated from these. The values of

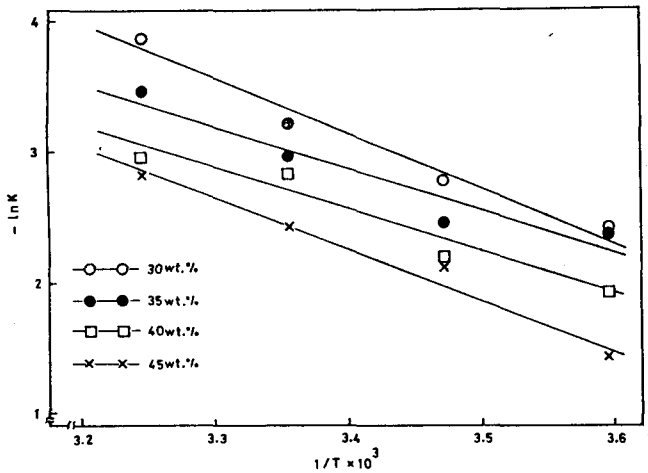

Figure 9. $-\ln K$ *vs.* $1/T$ for the corn starch-water suspensions.

Table 2. Thermodynamic Parameters Involved in Flow Units Transition for the Corn Starch-Water Suspensions

thermodynamic parameters / wt.%	ΔG^o_{298} (kcal mol^{-1})	ΔH^o (kcal mol^{-1})	ΔS^o_{298} (cal mol^{-1}K^{-1})
30	1.906	−8.045	−33.38
35	1.758	−6.230	−26.79
40	1.677	−6.313	−26.80
45	1.440	−7.527	−30.08

ΔG^o, ΔH^o and ΔS^o are summarized in Table 2.

Discussion

Thermodynamic Parameters for Flow Unit Transition. In Table 2, the enthalpy changes for the flow unit transition of the corn starch-water suspensions are ~−10 kcal/mol and these values correspond to the formation of hydrogen bond, as previously had been studied by Bang *et al.*.[11]

Also in Table 2, the free energy changes decrease with increasing the concentration. This means that hydrogen bond is strong in more concentrated system and thus the concentration of the flow unit 3 increases as compared with the lower concentrated system.

Ostwald Curve. The Ostwald curve has the following characteristics: (1) there is an inflection point in the linear plot of $\dot{s}$ *vs.* f (2) the part of the flow curve beyond the inflection point is extrapolated to the origin.

In 1957, Hahn *et al.*[5] had explained the Ostwald curve by the assumption: (1) there are at least two kinds of flow units, Newtonian and non-Newtonian (2) the non-Newtonian (entangled) units are transformed into the Newtonian (disentangled) units by stresses, eventually being completely changed to the Newtonian units by high stresses (by high shear rate) (3) the transformation is in kinetic equilibrium, the concentrations of the two kinds of flow units are time-independent. Umeya had also treated the Ostwald curves by separating with the specific regions, first Newtonian, pseudo-plastic,

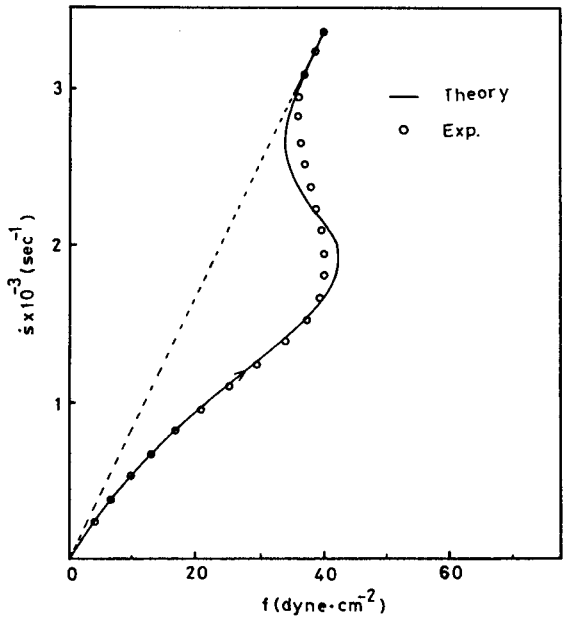

Figure 10. Flow curve of 35 wt.% potato starch-water suspension at 35 ℃.

dilatant and second Newtonian.[14]

Recently, we observed that for the 35 wt.% potato starch -water suspension at 35 ℃, the shape of the flow curve is very similar to the Ostwald curve in Figure 10. Using the following Eq. (28) which was introduced the relations, $\alpha_2\cong\alpha_3$, $\beta_2\cong\beta_3$ and $c_2\cong c_3$ to Eq. (22), we analyzed Figure 10.

$$f=\frac{X_1\beta_1}{\alpha_1}\dot{s}+\frac{1}{1+K\ \exp(c_0\dot{s}^2/RT)}\frac{1-X_1}{\alpha_2}\sinh^{-1}\{(\beta_2)_0\dot{s}\ \exp(c_2\dot{s}^2/RT)\}+\frac{K\ \exp(c_0\dot{s}^2/RT)}{1+K\ \exp(c_0\dot{s}^2/RT)}\frac{1-X_1}{\alpha_2}\sinh^{-1}\{(\beta_2)_0\dot{s}\ \exp(-c_2\dot{s}^2/RT)\} \quad (28)$$

The following values of the parameters involving in Eq. (28) were obtained: $K=1.334\times10^{-2}$, $c_0=6.530\times10^{-4}$, $X_1\beta_1/\alpha_1=1.183\times10^{-3}$, $(1-X_1)/\alpha_2=1.452$, $(\beta_2)_0=2.943\times10^{-3}$ and $c_2=3.312\times10^{-3}$. The theoretical curve in Figure 10 is obtained by calculations substituting the above values into Eq. (28). The agreement between theory and experiment is satisfactory. Thus, one notes that Eq. (28) can be applied to the Ostwald curve.

Stress Relaxation. The stress relaxation is one of the properties for visco-elastic solid materials and it signifies the phenomenon that the stress decreases with time at a fixed strain. Many investigators had described the stress relaxation by using some mechanical models[15] which combined spring and dash-pot, respectively meaning elasticity and viscosity. Similarly, the stress relaxation for non-solid materials points that the stress decrease with time at a same shear rate and it get to fixed value after long time.

Here, we suggest that Eq. (22) can be applied to the stress relaxation for non-solid materials. It is assumed that the stress relaxation is due to the flow unit transition with time. If the experimental condition, $\dot{s}=\rho(t_0+t)$ is introduced to the parts for the flow unit fraction of Eq. (22), Eq. (29) is obtained:

$$f=\frac{X_1\beta_1}{\alpha_1}\dot{s}+\frac{1}{1+K\ \exp\{c_0\rho^2(t_0+t)^2/RT\}}\frac{1-X_1}{\alpha_2}\sinh^{-1}\{(\beta_2)_0\dot{s}\ \exp(c_2\dot{s}^2/RT)\}+\frac{K\ \exp\{c_0\rho^2(t_0+t)^2/RT\}}{1+K\ \exp\{c_0\rho^2(t_0+t)^2/RT\}}\frac{1-X_1}{\alpha_3}\sinh^{-1}\{(\beta_3)_0\dot{s}\ \exp(-c_3\dot{s}^2/RT)\} \quad (29)$$

where t_0 is a lapse-time until the starting of stress relaxation, t is a working-time of stress relaxation, ρ is a coefficient which was related to the acceleration of shear rate and $\dot{s}$ is a constant shear rate at the condition of stress relaxation.

References

1. Hahn, S. J.; Ree T.; Eyring, H. *Ind. Eng. Chem.* **1959**, *51*, 856.
2. Chavan, V. V.; Desarkar, A. K.; Ulbrecht, J. *Chem. Eng. J.* **1975**, *10*, 205.
3. Glasstone, S.; Laidler, K. J.; Eyring, H. *The Theory of Rate Processes*; Hammet, S. P., Ed.; McGraw-Hill: New York and London, U.S.A. and U.K., 1941; Chapter 6.
4. Ree, T.; Eyring, H. *J. Appl. Phys.* **1955**, *26*, 793.
5. Hahn, S. J.; Ree, T.; Eyring, H. *NLGI Spokesman (Jour. Natl. Lubricating Grease Inst.)* **1957**, *21*, 12.
6. Park, K.; Ree, T. *J. Korean Chem. Soc.* **1971**, *15*, 293.
7. Utsugi, H.; Ree, T. *Advances Chem. Phys.* **1971**, *21*, 273.
8. Sohn, D. W.; Kim, E. R.; Hahn, S. J.; Ree, T. *Bull. Korean Chem. Soc.* **1986**, *7*, 257.
9. Hoffman, R. L. *J. Colloid Interface Sci.* **1974**, *46*, 491.
10. Kanno, T.; Wagatsuma, M.; Umeya, K. *Nippon Reoroji* **1976**, *4*, 170.
11. Bang, J. H.; Kim, E. R.; Hahn, S. J.; Ree, T. *Bull. Korean Chem. Soc.* **1983**, *4*, 212.
12. Green, H. *Industrial Rheology and Rheological Structures*; John Wiley & Sons, Inc.: New York, U.S.A., 1949; p. 143.
13. Utsugi, H.; Kim, K.; Ree, T.; Eyring, H. *NLGI Spokesman (Jour. Natl. Lubricating Grease Inst.)* **1961**, *25*, 125.
14. Umeya, K. *Proc. 5th Intern. Rheol. Congr.*; Onogi, S., Ed.; Uneversity of Tokyo Press: Tokyo, Japan, 1970; Vol. 2, p 295.
15. (a) Tovolsky, A. V.; Andrews, R. D. *J. Chem. Phys.* **1945**, *13*, 3. (b) Halsey, G.; White, H. J.; Eyring, H. *Text. Res. J.* **1945**, *15*, 295. (c) Chase, K. W.; Goldsmith, W. *Exp. Mech.* **1974**, *14*, 10. (d) Sadd, M. H.; Morris, D. H. *J. Appl. Polym. Sci.* **1976**, *20*, 421.